Ultimate Strength of Reinforced Concrete Members under Combined Loading

La résistance à la rupture d'éléments en béton armé sous charges combinées.

Traglast von Stahlbetonbauteilen unter kombinierten Belastung

RYOICHI SHOHARA
Research Engineer
Shimuzu Construction Co., Ltd.
Tokyo, Japan

BEN KATO
Prof. Dr.-Eng.
University of Tokyo
Tokyo, Japan

SUMMARY
The ultimate strength of reinforced concrete members is analyzed based on the concept of a diagonal compression field. In this analysis, the interaction among bending moment, axial force and shear force is evaluated using a simple mathematical model. This theory is very simple but can explain the resisting mechanisms of reinforced concrete beam-columns and of precast concrete connections by a unified theory. The theoretical predictions obtained here are compared with the test results of many beam-column specimens and with those of push-off specimens; a satisfactory agreement was found.

RÉSUMÉ
La résistance à la rupture d'éléments en béton armé est analysée sur base du principe de champs de compression diagonale. Dans cette étude, l'interaction entre moments de flexion, effort axial et effort de cisaillement est évaluée par un modèle mathématique simple. Bien que simple, cette théorie est capable d'expliquer conjointement les mécanismes de liaisons entre poutres et colonnes en béton armé et entre éléments préfabriqués. Les prédictions théoriques obtenues ici sont comparées aux résultats expérimentaux de jonctions poutres-colonnes et de joints entre éléments préfabriqués.

ZUSAMMENFASSUNG
Die Traglast von Stahlbetonbauteilen ist mithilfe des Konzepts des Diagonaldruckfeldes berechnet. Kombinationen von Biegemoment, Normalkraft und Querkraft wurden mit einem einfachen mathematischen Modell behandelt.
Ortbeton- und Fertigteilkonstruktionen können damit behandelt werden. Befriedigende Übereinstimmung zwischen Theorie und Versuch wurde gefunden.

1. INTRODUCTION

In the conventional evaluation of the ultimate strength of beam-columns subject to combined axial thrust, bending moment and shear, the moment capacity is evaluated considering the interaction with axial force firstly, and then the shear force is calculated from the moment diagram at ultimate state depending on the end condition of the members, and this shear force is compared with the maximum shear capacity of the members which is evaluated on the basis of failure modes of the member. In this procedure of estimating shear capacity, different mechanisms of shear transfer through a section are assumed corresponding to the observed failure modes such as diagonal shear failures and shear bond failure, where the interaction of the shear with axial force and/or beinding stress is not taken into account. Since the observation of ultimate strength and failure mode in shear is made on the limited number of test specimens and thus of the limited varieties of parameters, there is a vulnerability of overlooking other possible modes of failure unless the assessment should be made on the basis of a comprehensive resisting mechanism of the member against axial force, bending moment and shear force.

Herein, a structural model is developed on the basis of the compression field concept. And the ultimate strengths of various types of reinforced concrete members such as beam-columns, beams and precast concrete connections are analyzed in the unified theoretical approach, taking the full interaction among performances of shear, bending and axial force into account.

The theoretical predictions obtained herein are compared with the test results consisting of many beam-column specimens and push-off specimens to show a satisfactory agreement each other.

2. ANALYSIS

The ultimate load carrying capacities of reinforced concrete members are analyzed. In this structural model, the equilibrium is secured through the entire member and the stresses in any constituent elements do not exceed their ultimate stresses, but the compatibility of strains and deformation is not necessarily satisfied. Therefore the lower bound solution will be obtained from this analysis. The stress-strain relationship of steel is assumed to be elastic-perfectly plastic ignoring the effect of strain-hardening. As for that of concrete, it is assumed that the concrete has no resistance against tension and that it can develop some extent of plastic deformation keeping its maximum stress against compression.

2.1. Ultimate Strength of Reinforced Concrete Beam-column Subject to Anti-symmetrical Bending

In this paragraph the ultimate loading capacity of a reinforced concrete beam-column subject to anti-symmetrical bending at its ends under constant axial force is analyzed.

A reinforced concrete beam-column in this model is fictitiously divided into two systems, namely web reinforcement and the diagonal compression field system, and the consisting materials are allocated into these systems without overlapping.

The loading condition and the dimensions of various parts of the reinforced concrete column to be analyzed are shown in Fig.1, where the symbols are;

N = constant axial force
M = bending moment
Q = shearing force
ℓ = length of the member
D = depth of the section
b = width of the section
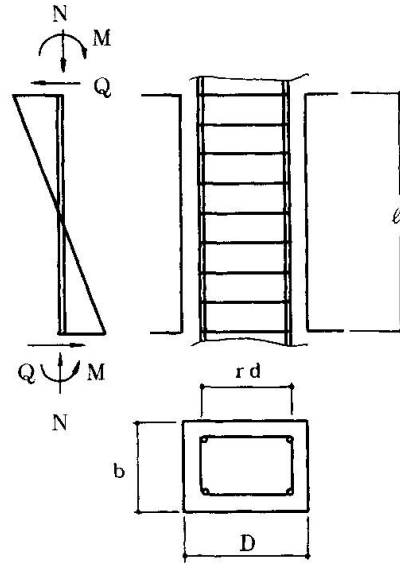$_r$d = distance between the center of gravities of reinforcing bars at each side

Fig.1 Reinforced Concrete Member and Loading Condition

2.1.1. Bending Moment and Shear Force Carried by the Web Reinforcement System

A kind of truss mechanism consisting of web reinforcement, main reinforcement and concrete which resists compression force are assumed as a load carrying mechanism. The concrete is divided into virtual discreet elements with their inclinations $\varphi = 45°$, their stresses Fc, and imaginary width of the concrete βb in equilibrium with the stresses of the reinforcements.

Assuming the stress of main reinforcing bars at each end of the member $T = \alpha T_y$ when the web reinforcing bars have yielded, the following equations are derived from the equilibrium of the system. Where $T_y = {}_r a \cdot {}_r \sigma_y$ is the yield strength of the reinforcing bars at one side of the section.

$$_wQ = P_w \cdot {}_w \sigma_y \cdot b \cdot {}_r d \tag{1}$$

$$_wM = \alpha T_y \cdot {}_r d \tag{2}$$

$$_wN = {}_wQ \tag{3}$$

$$\alpha = \frac{P_w \cdot {}_w \sigma_y \cdot b \cdot \ell}{2T_y}$$

$$\beta = \frac{2 P_w \cdot {}_w \sigma_y}{F_c} \quad (0 \leq \alpha, \beta \leq 1)$$

where;

$_r a$ = total sectional area of main reinforcing bars allocated on either side of the section with respect to the bending axis

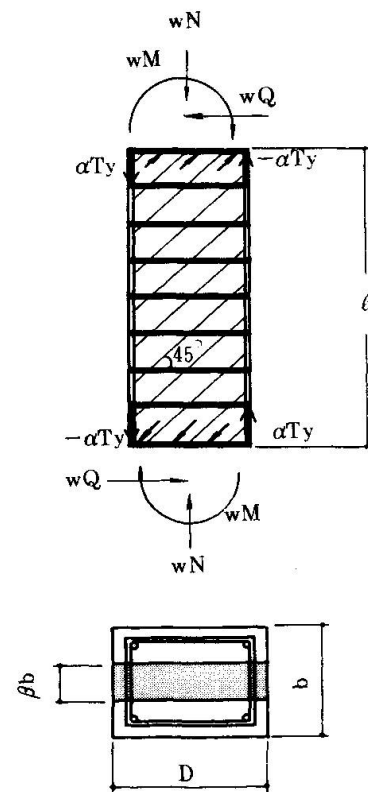$_w a$ = sectional area of a set of web reinforcing bars

Fig.2 Equilibrium of Web Reinforcement System

Pw = web reinforcement ratio $\frac{w^a}{bx}$

X = pitch of web reinforcing bars

$_r\sigma y$ = yield point of main reinforcement

$_w\sigma y$ = yield point of web reinforcement

F_c = maximum compressive stress of concrete

Putting $\alpha = 1$ in the above equations, it can be observed that the yielding of web reinforcement and that of main reinforcement will take place simultaneously when the condition that

$$\overline{P}_w = \frac{2_r a \cdot _r\sigma y}{b\ell \cdot _w\sigma y}$$

is satisfied. And it will be seen that the moment capacity of this system will be saturated at this state, and does not increase further even if one provides more amount of web reinforcement than that defined by the critical value of $\overline{P}w$.

In general, the main reinforcements have reserve strength of $(1-\alpha)Ty$ before yielding.

2.1.2. Bending Moment and Shear Force Carried by the Compression Field

At this step of the analysis, the materials in the member which can be utilized as load carrying elements are $(1-\alpha)_r a$ of the main reinforcement and the concrete. Compression field which consists of these materials are assumed as shown Fig.3(a), where c corresponds a steel chord member consisting of $(1-\alpha)_r a$, and d is a fictitious compressive diagonal member made of concrete.

In Fig.3(a), dashed lines which define the fictitious diagonal compression member d are drawn from the corners of the opposite column ends with a inclination θ which is the function of $_tM$ and $_tN$, and the width of the horizontal intersection of this diagonal member is $X = D - \ell \tan\theta$.

Denoting the compressive stress in this diagonal member σ_c, the compressive force in this member N_c can be written as

$$N_c = \sigma_c b' \cdot X \cdot \cos\theta$$
$$= (D - \ell \tan\theta)b' \cdot \sigma_c \cdot \cos\theta \qquad (4)$$

where $b' = (1-\beta)b$ is fictitious width of diagonal compression field.

The equilibrium of the axial force, the bending moment and the shear at each end of the member can be written as follows.

$$_tN + 2S = N_c \cdot \cos\theta \qquad (5)$$
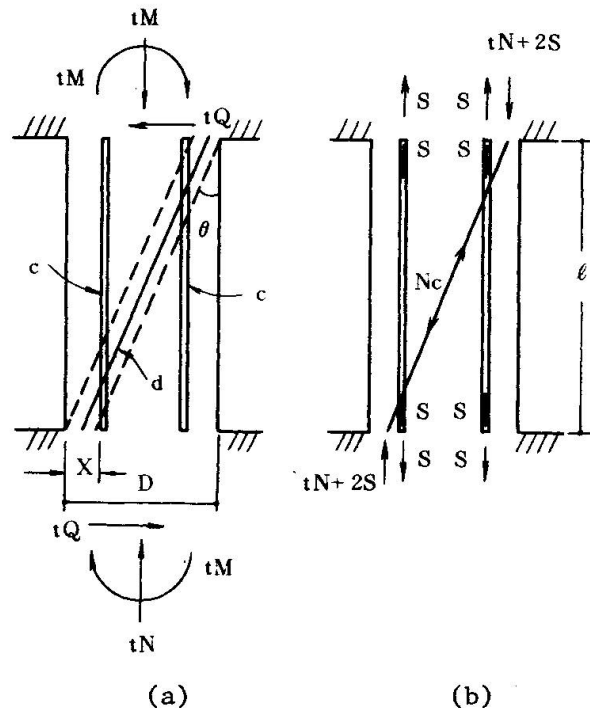

(a)   (b)

Fig.3 Compression Field Model Subject to Anti-symmetrical Bending

$$tM = \frac{\ell \cdot \tan\theta \cdot N_c \cdot \cos\theta}{2} = \frac{N_c \cdot \ell \cdot \sin\theta}{2} \tag{6}$$

$$tQ = N_c \cdot \sin\theta \tag{7}$$

Where $tN = N - wN$ is the axial force carried by this compression field system and is positive for compression, tM is the bending moment at each end of the member and is positive for clockwise direction, tQ is the shear force, and the cords forces S are positive for tension. Substituting Eq.(4) into Eq.(5), the inclination of the diagonal compression field $\tan\theta$ is found to be

$$\tan\theta = \frac{\lambda}{2} \left(\frac{b' D \cdot \sigma_c}{2S + tN} \right) \left\{ \sqrt{1 + \frac{4}{\lambda^2} \left(\frac{2S + tN}{b' D \cdot \sigma_c} \right) \left(1 - \frac{2S + tN}{b' D \cdot \sigma_c} \right)} - 1 \right\}. \tag{8}$$

where $\lambda = \ell/D$, and substituting Eqs.(4) and (8) into Eq.(6), the end moment tM is found to be

$$tM = \frac{b' D \cdot \sigma_c \lambda \ell}{4} \left\{ \sqrt{1 + \frac{4}{\lambda^2} \left(\frac{2S + tN}{b' D \cdot \sigma_c} \right) \left(1 - \frac{2S + tN}{b' D \cdot \sigma_c} \right)} - 1 \right\}. \tag{9}$$

Eq.(9) shows that tM increases when σ_c increases, and tM becomes maximum when σ_c becomes its maximum value F_c, and if $2S + tN \leq \frac{bD \cdot \sigma_c}{2}$, tM becomes maximum when the chords forces S reach their yield value S_o, namely

$$S = S_o = (1 - \alpha)T_y .$$

Region I $tN < N_1$, $N_1 = \frac{N_o}{2} - 2S$.

Substituting F_c into Eq.(9) for σ_c, and S_o for S, the maximum bending moment at column ends is found to be

$$tM = \frac{N_o \lambda \ell}{4} \left\{ \sqrt{1 + \frac{4}{\lambda^2} \left(\frac{2S_o + tN}{N_o} \right) \left(1 - \frac{2S_o + tN}{N_o} \right)} - 1 \right\}. \tag{10}$$

Where; $N_o = b' D F_c$ = maximum compressive capacity of the concrete section used in compression field system. And the corresponding shear force tQ is

$$tQ = \frac{2 tM}{\ell} = \frac{N_o \lambda}{2} \left\{ \sqrt{1 + \frac{4}{\lambda^2} \left(\frac{2S_o + tN}{N_o} \right) \left(1 - \frac{2S_o + tN}{N_o} \right)} - 1 \right\}. \tag{11}$$

Looking into the effect of the axial force tN on the moment capacity through Eq.(10), it can be seen that tM takes its maximum when tN reaches $N_1 = (N_o/2) - 2S_o$, and until tN reaches this critical value of N_1, tM increases with the increase of tN. Substituting $N_1 = (N_o/2) - 2S_o$ into Eqs. (10) and (11) for tN, the bending moment and shear force under this critical axial force are found to be

$$tM_1 = \frac{1}{4} N_o \ell \left(\sqrt{\lambda^2 + 1} - \lambda \right) \tag{12}$$

$$tQ_1 = \frac{1}{2} N_o \left(\sqrt{\lambda^2 + 1} - \lambda \right). \tag{13}$$

And the inclination of the diagonal at this state is

$$\tan\theta_1 = \sqrt{\lambda^2 + 1} - \lambda . \tag{14}$$

When the axial force is not larger than this critical value N_1, both steels and concrete develop their full capacity at the ultimate state, and this mode of failure can be defined as the flexural failure in a broad sense.

Region II. $N_1 <_t N < N_2$ $N_2 = \dfrac{N_0}{2} + 2S_0$

According to Eq.(10), the bending moment reaches the maximum value at the critical axial force N_1, and then decreases for the larger axial force, and correspondingly the inclination θ starts to decrease as can be seen from Eq.(8). However this is not the only way of excurtion. As Eq.(8) and (9) are the function of $(2S + N)$ and not the independent function of S or N, both $_t M$ and θ can remain unchanged for the axial force which is larger than N_1 if S decreases and goes back into the elastic region. And since the member should develop its maximum resistance against given external forces according to the lower bound theorem, this behavior must be the actual one. N-S relationship for this transitive region can be written as

$$2S + {_t N} = 2S_0 + {_t N} = \dfrac{N_0}{2} . \tag{15}$$

From this equation, it can be seen that S becomes zero at the axial force $N_0/2$, and the chord stress will change its sign into compression when the axial force exceeds this value, and finally the chords will yield by compression when the axial force reaches

$$N_2 = \dfrac{N_0}{2} + 2S_0 . \tag{16}$$

Thus it can be concluded that, for the region of $N_1 <_t N < N_2$, the ultimate strength of the member is governed by the compressive failure of the concrete diagonal, while the chord members remain elastic. For the range of this axial force, $_t M_1$, $_t Q_1$ and θ_1 keep constant values, and they are given by Eqs.(12), (13) and (14) respectively. This mode of failure can be defined as the shear failure.

Region III. $N_2 \leq_t N \leq N_3$, $N_3 = N_0 + 2S_0$

Since the only difference of equilibrium conditions between Region I and Region III is that S_0 in the former becomes $-S_0$ in the latter, $_t M$ and $_t Q$ for Region III can be obtained by replacing S_0 in Eqs(10) and (11) by $-S_0$ as

$$_t M = \dfrac{1}{4} N_0 \lambda \ell \left\{ \sqrt{1 + \dfrac{4}{\lambda^2} (\dfrac{{_t N} - 2S_0}{N_0}) (1 - \dfrac{{_t N} - 2S_0}{N_0})} - 1 \right\} \tag{17}$$

$$_t Q = \dfrac{2\,_t M}{\ell} = \dfrac{1}{2} N_0 \lambda \left\{ \sqrt{1 + \dfrac{4}{\lambda^2} (\dfrac{{_t N} - 2S_0}{N_0}) (1 - \dfrac{{_t N} - 2S_0}{N_0})} - 1 \right\} . \tag{18}$$

Eq.(17) shows that $_t M$ decreases with increasing value of $_t N$. As the extreme, $_t M$ becomes zero when the axial force reaches the following value

$$N_3 = N_0 + 2S_0 . \tag{19}$$

N_3 is the sum of the axial yield force of concrete and that of steel chord parts. The failure mode in this region can also be defined as the flexural failure.

The case for $\alpha = 1$

This case corresponds to the situation of $S=0$ in the preceding section. Since the description for the Region I in the preceding section is independent of the value of S or S_O, the moment and shear capacities for this region can be obtained by introducing $S_O=0$ into Eqs.(10) and (11) as

$$_tM = \frac{1}{4} N_O\lambda\ell\left\{ \sqrt{1 + \frac{4}{\lambda^2} (\frac{tN}{N_O}) (1 - \frac{tN}{N_O})} - 1\right\} \qquad (20)$$

$$_tQ = \frac{1}{2} N_O\lambda\left\{ \sqrt{1 + \frac{4}{\lambda^2} (\frac{tN}{N_O}) (1 - \frac{tN}{N_O})} - 1\right\} . \qquad (21)$$

The critical axial force which makes the moment maximum also can be found by placing $S_O=0$ in the expression of N_1 as

$$N_1' = \frac{N_O}{2} .$$

The maximum values of $_tM$ and $_tQ$ for this critical axial force are independent of the value of S_O and are given by Eqs.(12) and (13) of the preceding section.

When $S=0$, from Eqs.(20) and (21), it can be seen that it is impossible to keep $_tM$ and $_tQ$ unchanged for the increasing value of $_tN$. Therefore, the Region II does not exist, namely the shear failure does not occur in this case. And therefore, Eqs.(20) and (21) are valid even for the larger axial force than N_1', and eventually $_tM$ becomes zero when the axial force reaches $N_3'= N_O$.

2.1.3. Total Capacity

The total bending capacity of a member is obtained by summing up those of web reinforcement system (section 2.1.1.) and of compression field (section 2.1.2.). The result is summerized in the following;

Region I. $_tN \leq N_1$, $N_1 = \frac{N_O}{2} - 2S_O$

$$M = _wM + \frac{1}{4} N_O\lambda\ell\left\{ \sqrt{1 + \frac{4}{\lambda^2} (\frac{2S_O+tN}{N_O}) (1 - \frac{2S_O+tN}{N_O})} - 1\right\} \qquad (22)$$

$_wM = \alpha \cdot _ra \cdot _r\sigma y \cdot _rd$, $\alpha = (P_w \cdot \sigma_y \cdot b\ell)/(2_ra \cdot _r\sigma y) \leq 1$

$_tN = N - _wN$, $_wN = _wQ$.

Region II. $N_1 < _tN < N_2$, $N_2 = \frac{N_O}{2} + 2S_O$.

$$M = _wM + \frac{1}{4} N_O\ell (\sqrt{\lambda^2 + 1} - \lambda) . \qquad (23)$$

Region III. $N_2 \leq {}_tN \leq N_3$, $N_3 = N_0 + 2S_0$

$$M = {}_wM + \frac{1}{4} N_0 \lambda \ell \left\{ \sqrt{1 + \frac{4}{\lambda^2} (\frac{{}_tN - 2S_0}{N_0})(1 - \frac{{}_tN - 2S_0}{N_0})} - 1 \right\}. \quad (24)$$

2.2. Ultimate Strength of Reinforced Concrete Beam-column Subject to Simple Beam Type Loading

Considerable number of specimens have been tested under simple beam type loading, and according to these experimental results[1] the strength of a simple-beam type specimen differs considerably from that of the specimen subject to anti-symmetrical bending. For these reasons, the ultimate strength of a reinforced concrete beam-column subject to simple-beam type loading is analyzed here. Of cource, equations obtained here can directly be applied to symple-beam or cantilever type structures.

To begin with, characteristics of these two loading systems are discussed qualitatively referring to Fig.4.

As for the specimen subject to anti-symmetrical bending, the imaginary diagonal compression field could touch point A to carry larger shear force. On the other hand, as for a simple beam type specimen, it is impossible the diagonal compression field to touch the point A unless sufficient main reinforcing bars are provided to counterbalance the bending moment produced by the compression stress of the diagonal member, because at point A the boundary condition of bending moment is $M = 0$.

On this reason, if the lengths of the members and other dimensions are equal, ultimate shear strength of the specimen subject to anti-symmetrical bending is larger than that of the specimen subject to simple-beam type loading unless main reinforcing bars are not sufficiently provided to the specimen.
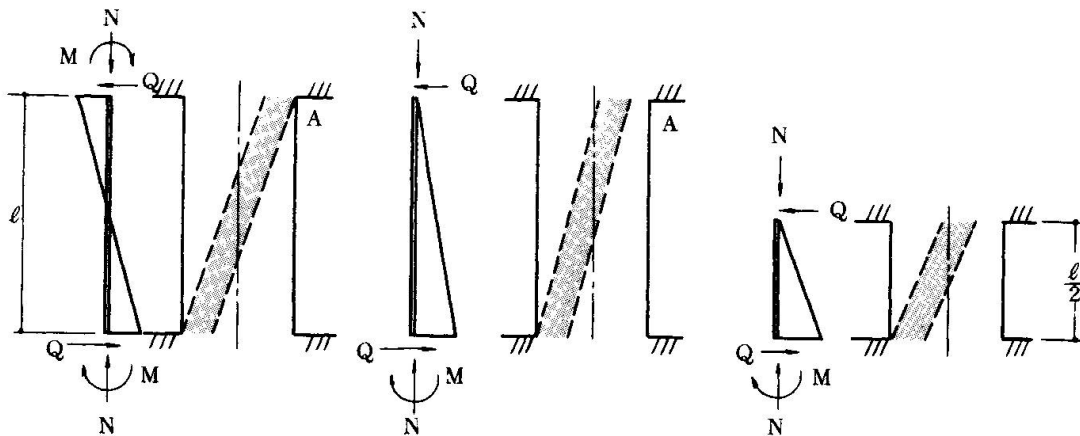
(a) Beam-column under Anti-symmetrical Bending (b) Beam-column under Simple Beam Type Loading (c) Simple Beam Type Specimen with Same Parameter M/QD to Fig.4(a)

Fig.4 Predicted Inclinations of the Diagonal Compression Fields Corresponding to the Various Loading Systems

Figs.4(a) and (c) show the differences of models under the same condition of the parameter M/QD. Under this condition a simple beam type specimen carry larger shear than that of the specimen subject to anti-symmetrical bending with equal dimensions, because the compression field of the former can be drawn nearer to the edge of the section at point $M = 0$ corresponding to the amount of the main reinforcing bars, while that of the latter always remains at the center of the section.

2.2.1. Bending Moment and Shear Force Carried by Web Reinforcement System

According to the same method descrived in section 2.1.1., the ultimate loading capacity of a web reinforcement system is deduced with the same equations (1), (2) and (3), though under this loading condition $\alpha = P_w \cdot w\sigma_y \cdot b\ell/T_y$. Because the relationship $_wM = \ell \cdot _wQ$ exists while in section 2.1.1. $_wM = \ell \cdot _wQ/2$.

2.2.2. Bending Moment and Shear Force Carried by the Compression Field

Based on the boundary condition $M = 0$ at point A and the equilibrium of forces, referring to Fig. 5(a), the bending moment at point B can be derived as follows.

$$_tM = \lambda N_0 \cdot \ell \left\{ \sqrt{1 + \frac{(_tN + S + S')N_0 + \gamma(S - S')N_0 - (_tN + S + S')^2}{(\lambda N_0)^2}} - 1 \right\} \quad (25)$$

and the corresponding shear force across the section is

$$_tQ = {_tM}/\ell .$$

where; $\gamma = _rd/D$

According to the lower bound theorem, chord forces S and S' which maximize the moment $_tM$ should be obtained. The derived equations are as follows.

Region	I	$_tN \leq \dfrac{1-\gamma}{2} N_0 - 2S_0$	$S = S_0, \quad S' = S_0$
Region	II	$\dfrac{1-\gamma}{2} N_0 - 2S_0 < {_tN} \leq \dfrac{1-\gamma}{2} N_0$	$S = S_0, \quad S' = \dfrac{1-\gamma}{2} N_0 - S_0 - {_tN}$
Region	III	$\dfrac{1-\gamma}{2} N_0 < {_tN} \leq \dfrac{1+\gamma}{2} N_0$	$S = S_0, \quad S' = -S_0$
Region	IV	$\dfrac{1+\gamma}{2} N_0 < {_tN} \leq \dfrac{1+\gamma}{2} N_0 + 2S_0$	$S = \dfrac{1+\gamma}{2} N_0 + S_0 - {_tN}, \quad S' = -S_0$
Region	V	$\dfrac{1+\gamma}{2} N_0 + 2S_0 < {_tN}$	$S = -S_0, \quad S' = -S_0$

As the compression field can not protrude beyond member width, following condition must be satisfied.

$$_tN^2 - [N_0 - 2(S+S')] {_tN} - (S+S')N_0 + (S-S')\gamma N_0 + \frac{(S-S')^2}{\lambda'^2} + (S+S')^2 \leq 0 \quad (26)$$

where; $\lambda' = \ell/_rd$

If this condition is not satisfied, a model where the compression field touches point A is supposed as shown in Fig.5(b). Satisfying the boundary condition and the equilibrium of forces of this model, the bending moment at point B $_tM$ is derived as follows.
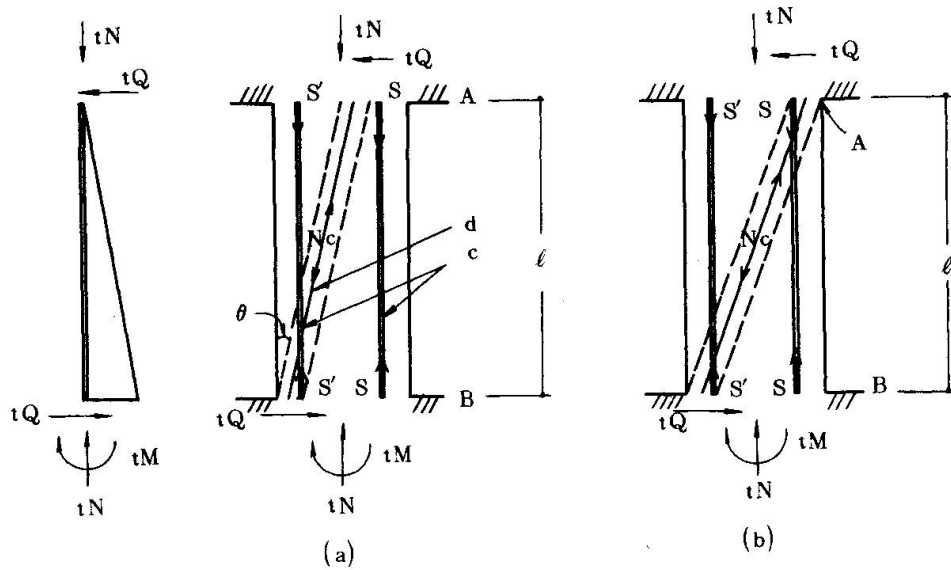
Fig.5 Equilibrium of Compression Field Model Subject to Simple Beam Type
        Loading

$$_tM = N_0 \cdot \ell \ \frac{\tan\theta}{1 + \tan^2\theta} \ (1 - \lambda\tan\theta) \tag{27}$$

The inclination of the diagonal compression field $\tan\theta$ which maximize $_tM$ can be obtained by the following equations.

Region VI $_tN \leq \dfrac{N_0}{2} \ [\ 1 + \lambda' \ (\sqrt{\lambda^2 + 1} \ - \lambda \ ) \ ] - 2S_0$.

$$\tan\theta = \frac{N_0(\lambda'-\lambda)}{2(N_0\lambda\lambda'+2S_0+_tN)} \left\{ \sqrt{1 + \frac{4(N_0\lambda\lambda'+2S_0+_tN)(N_0-2S_0-_tN)}{N_0^2 \ (\lambda-\lambda')^2}} + 1 \right\} \tag{28}$$

Region VII $\dfrac{N_0}{2} \ [\ 1+\lambda' \ (\sqrt{\lambda^2+1} \ - \lambda) \ ] - 2S_0 < \ _tN < \dfrac{N_0}{2} \ [\ 1-\lambda'(\sqrt{\lambda^2+1} \ -\lambda)\ ] + 2S_0$

$$\tan\theta = \sqrt{\lambda^2 + 1} - \lambda \tag{29}$$

Region VIII $_tN \geq \dfrac{N_0}{2} [\ 1 - \lambda'(\sqrt{\lambda^2 + 1} \ - \lambda\ )] + 2S_0$

$$\tan\theta = \frac{N_0(\lambda'+\lambda)}{2(N_0\lambda\lambda'+2S_0-_tN)} \left\{ -\sqrt{1 - \frac{4(N_0\lambda\lambda'+2S_0-_tN)(N_0+2S_0-_tN)}{N_0^2 \ (\lambda+\lambda')^2}} + 1 \right\} \tag{30}$$

Loading capacities on these regions are obtained substituting above descrived values for $\tan\theta$ into Eq.(27).

In region VII the ultimate strength of the member is governed by the compressive failure of the concrete diagonal, while the chord members remain elastic. This mode of failure can be difined as the shear failure. For the range of axial force in region VII $_tM$ and $_tQ$ keep constant values as follows.

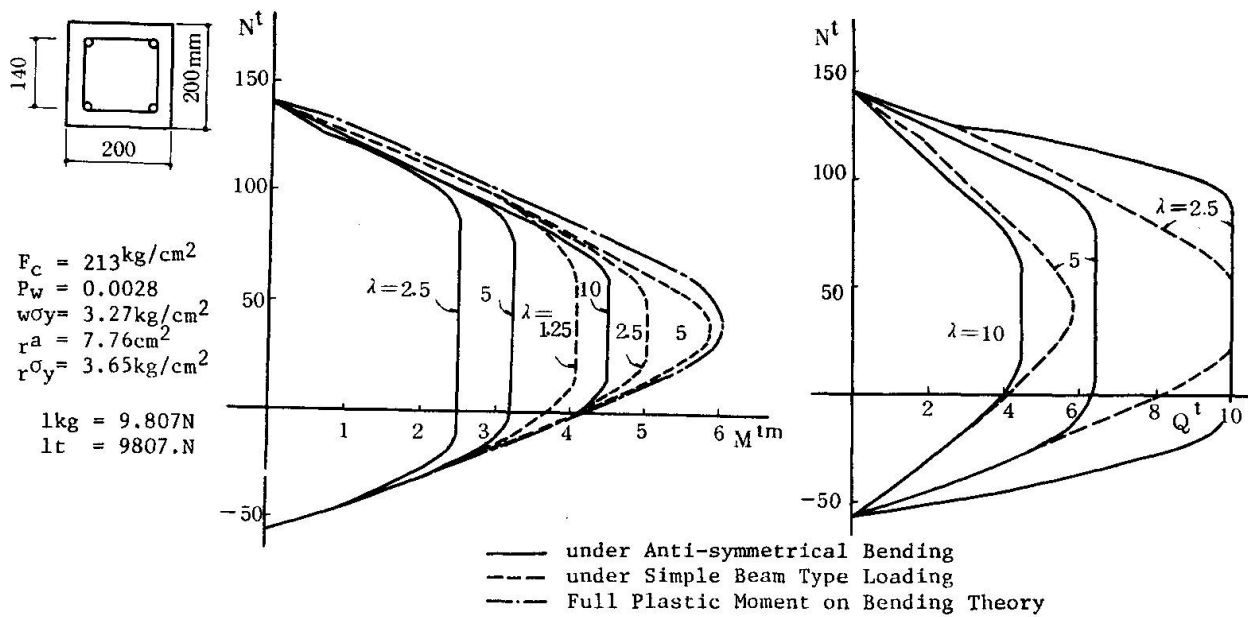$$_tM = \frac{N_0 \cdot \ell}{2} (\sqrt{\lambda^2 + 1} - \lambda) \qquad\qquad (31)$$

$$_tQ = \frac{N_0}{2} (\sqrt{\lambda^2 + 1} - \lambda) \qquad\qquad (32)$$

This region corresponds to region II in section 2.1.2.

2.2.4. Example

M - N interactions and Q - N interactions of reinforced concrete beam-columns with the section as shown in Fig.6(a) are shown in Figs.6(b) and (c) respectively evaluated according to the foregoing analysis.

According to this analysis, as parameter ℓ/D increases, the ultimate end moment M increases and "shear failure" region where moment capacity keep a constant value for the change of axial force N decreases. Referring to Fig.6(c), it can be understood that the ultimate shear capacity of the specimen subject to anti-symmetrical bending is larger than that subject to simple beam type loading with equal values of $\lambda(\ell/D)$.

$F_c = 213^{kg/cm^2}$
$P_w = 0.0028$
$_w\sigma_y = 3.27 kg/cm^2$
$_r a = 7.76 cm^2$
$_r\sigma_y = 3.65 kg/cm^2$

$1 kg = 9.807 N$
$1 t = 9807. N$

——— under Anti-symmetrical Bending
— — — under Simple Beam Type Loading
——·— Full Plastic Moment on Bending Theory

(a) Sample Section (b) M - N Interaction Curve   (c) Q - N Interaction Curve

Fig.6 Example

2.3. Ultimate Strength of a Reinforced Concrete Member Subject to Shear and Axial Force without Bending

Mattock et.al.[2] investigated the shear transfer strength of push-off specimens shown in Fig.7 supposing the shear transfer mechanism of precast concrete connections. The shear strength of such a reinforced concrete member subject to shear and axial force without bending is analyzed here making use of the analogical concept of diagonal compression field model for a beam-column descrived in section 2.1.2.

The specimen shown in Fig.7(a) corresponds to the beam-column shown in Fig.3 making the length of it sufficiently small. X - X' axis in Fig.7 corresponds to the longitidinal axis of the beam-column shown in Fig.3. The main reinforcing bars in Fig.3 correspond to the shear reinforcing bars shown in Fig.7.

The equations (11), (13) and (18) can be transformed into (33), (34) and (35) substituting $N_0 = bD \cdot F_c$, $_tN = bD\sigma_0$, $_tQ = \tau_u bD$, and $2S_0 = P_s \cdot \sigma_y \cdot bD$ and also replacing $\lambda = \ell/D$ by 0. Where;

σ_0 : mean value of compressive stress on the shear plane

τ_u : mean value of ultimate shear stress on the shear plane

P_s : shear reinforcement ratio

σ_y : yield point of reinforcement

Eqs.(33), (34) and (35) are thus derived equations to calculate the ultimate shear strength and the corresponding inclination of the diagonal for reinforced concrete member subject to shear and axial force without bending.

Push-off Specimen   Modified Push-off
                     Specimen

Fig.7 Loading Systems

Region I $\sigma_0 \leq \dfrac{F_c}{2} - P_s \cdot \sigma_y$

$$\tau_u = (P_s \cdot \sigma_y + \sigma_0) \cdot \sqrt{\dfrac{F_c}{P_s \cdot \sigma_y + \sigma_0} - 1}$$ (33)

$$\tan\theta = \sqrt{\dfrac{F_c}{P_s \cdot \sigma_y + \sigma_0}}$$

Region II $\dfrac{F_c}{2} - P_s \cdot \sigma_y < \sigma_0 \leq \dfrac{F_c}{2} + P_s \sigma_y$

$$\tau_u = \dfrac{F_c}{2}$$ (34)

$$\tan\theta = 1$$

Region III $\sigma_0 > \dfrac{F_c}{2} + P_s \cdot \sigma_y$

$$\tau_u = (-P_s \cdot \sigma_y + \sigma_0) \cdot \sqrt{\dfrac{F_c}{-P_s \cdot \sigma_y + \sigma_0} - 1}$$ (35)

$$\tan\theta = \sqrt{\dfrac{F_c}{-P_s \cdot \sigma_y + \sigma_0} - 1}$$

As shown in Fig.3 main reinforcing bars of the beam-column are located at each side of the section, while in the specimen shown in Fig.7 reinforcing bars are uniformly distributed. Yet, the strength is not affected with the locations of reinforcements as can be understood in Eq.(9). For this reason the substitution $2S_0 = P_s \cdot \sigma_y \cdot bD$ is capable.

As mentioned in section 2.1.2. reinforcements yield by tension in region I, by compression in region III while they remain elastic in region II.
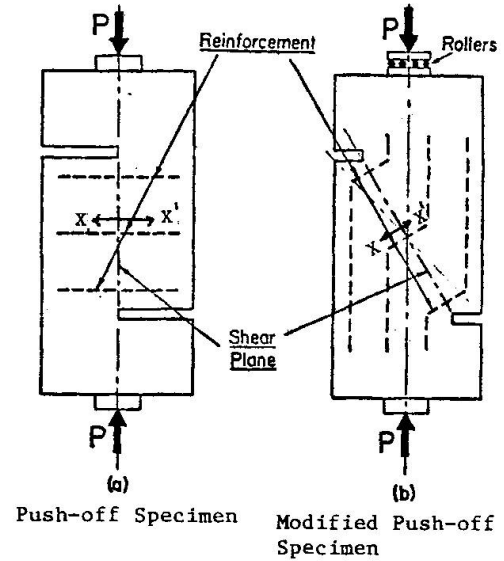
3. EXPERIMENTAL VERIFICATIONS

3.1. Strength of Reinforced Concrete Beam-columns

The prediction on this analysis are compared with experimental results of 877 beam-column specimens tested recently in Japan[1]

The experimental results of the specimens subject to anti-symmetrical bending in region II are compared with the prediction in Fig.8. As the vertical axis of Fig.8 shows the strength of the diagonal compression field, the modified experimental value Q_e' is computed by substructing the value $_wQ$ calculated with Eq.(1) from the experimental value Q_e. The experimental results agree satisfactory with the predicted tendency that the shear strength increases, as the paramater ℓ/D decrease.

All the specimens in region II are reported as shear failure from the experimentalists, though all the reported shear failure specimens are not in region II, but also scattered in the neighbourhood of region II. Main reason of this fact is supposed that they call it shear failure even if main reinforcing bars have yielded.

The ratios of experimental values Q_e to theoretical values Q_c are shown in Fig.9 ~ Fig.14 as to all the beam-column specimens, with the parameters ℓ/D and F_c. In table 1, mean values m and coefficients of variation σ/m concerning Q_e/Q_c are shown. Also in table 1 these values of empirical equations (36) and (37) for shear failure specimens, and Eq.(38) for flexure failure specimens are shown. These equations are commonly used in Japan[3].

$$Q_u = \left\{ (0.9 + \frac{\sigma_0}{250}) \ \frac{0.23 k_u k_p (F_c + 180)}{h_0/d + 0.23} \right.$$

$$\left. + 2.7 \sqrt{P_w \cdot_w \sigma_y} \right\} \cdot bj \qquad (36)$$

$$Q_u = \left\{ \frac{0.23 k_u k_p (F_c + 180)}{h_0/d + 0.23} + 0.1 \sigma_0 \right.$$

$$\left. + 2.7 \sqrt{P_w \cdot_w \sigma_y} \right\} \cdot bj \qquad (37)$$

Table 1 Comparison between Culculated and Experimental values

Beam-columns subject to Anti-symmetrical Bending

1 Shear Failure Specimens				
	Beam(112)		Column(57)	
	m	σ/m	m	σ/m
Writers	0.941	0.155	1.057	0.178
Eq.(36)	1.083	0.165	0.994	0.199
Eq.(37)	0.975	0.165	0.949	0.160

2 Flexure Failure Specimens				
	Beam(35)		Column(231)	
	m	σ/m	m	σ/m
Writers	1.149	0.121	1.096	0.118
Eq.(38)	1.099	0.131	1.008	0.104

3 Bond Failure Specimens (32)		
	m	σ/m
Writers	0.938	0.099
Eq.(36)	0.862	0.145
Eq.(38)	0.857	0.113

m ; mean value
σ/m ; coefficient of variation

Simple Beam Type Specimens

1 Shear Failure Specimens				
	Beam(45)		Column(119)	
	m	σ/m	m	σ/m
Writers	0.858	0.150	1.069	0.133
Eq.(36)	0.944	0.160	0.840	0.137
Eq.(37)	0.850	0.160	0.860	0.110

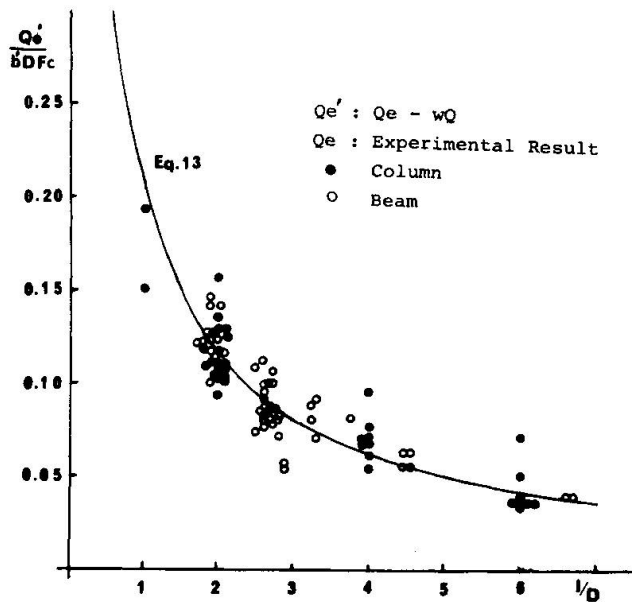| 2 Flexure Failure Specimens				
	Beam(94)		Column(152)	
	m	σ/m	m	σ/m
Writers	1.178	0.146	1.179	0.128
Eq.(38)	1.202	0.183	1.081	0.152

Fig.8 Comparison between Tests and Theory on Specimens Subject to Anti-symmetrical Bending in Region II

$$M_u = 0.8_r a \cdot_r \sigma_y \cdot D$$

$$+ 0.5\sigma_0 \cdot bD^2 (1 - \frac{\sigma_0}{F_c})$$

$$(38)$$

Where;

ku, kp = coefficients depending on the size of section and tensile reinforcement ratio respectively

h_0 = shear span

d = distance from extreme compression fiber to centroid of tension reinforcement

j = distance between the centroid of compression and tension stress

In this section a shear failure specimen is defined as the specimen reported as shear failure from the experimentalist and of which ultimate strength does not reach its ultimate flexure strength calculated by Eq.(38).

Seeing the above mentioned comparisons between experimental and theoretical values following facts are evident.

1) This analysis predicts the ultimate strength of shear failure specimens with equal accuracy as those of the empirical equations (36) and (37), and predicts the ultimate strength of flexure failure specimen a little conservatively, however coefficients of variation σ/m of this analysis for Q_e/Q_c are almost equal with those of Eq.(38).

2) This analysis predicts the ultimate strength of the specimens subject to anti-symmetrical bending and simple beam type loading with almost equal accuracy. Therefore the modelings on this theory as to the characteristics of each loading systems are supposed to be appropriate.
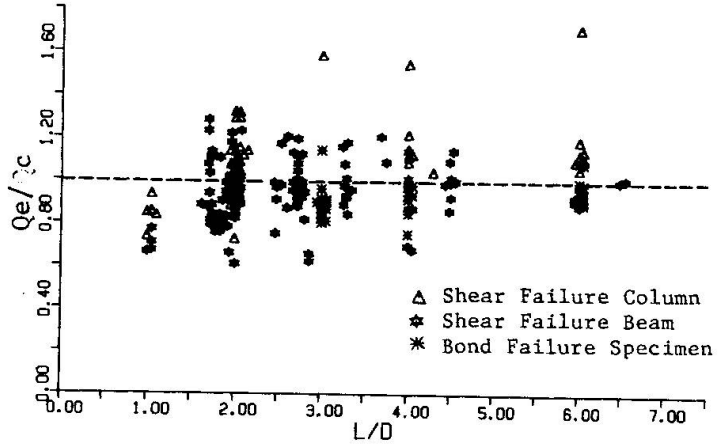

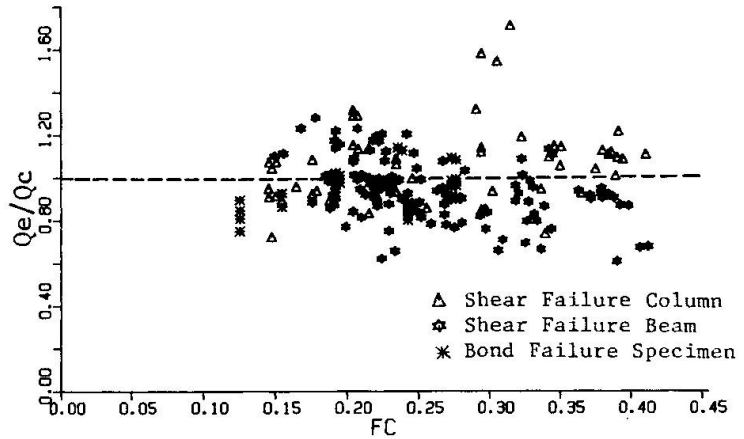Fig.9 Shear and Bond Failure Specimens Subject to Anti-symmetrical Bending

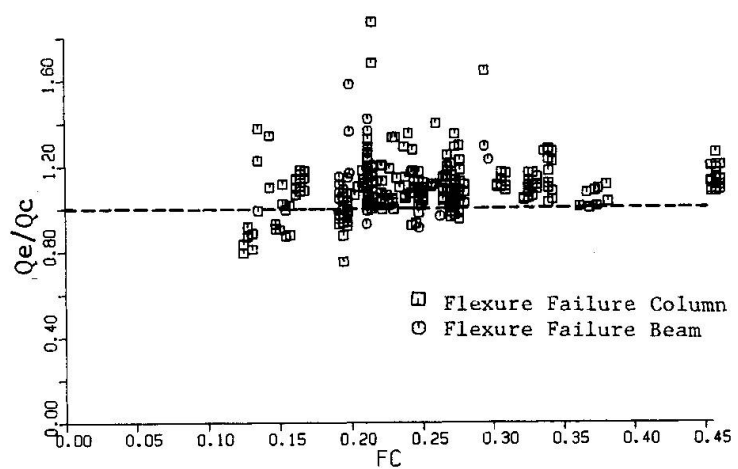Fig.10 Shear and Bond Failure Specimens Subject to Anti-symmetrical Bending

Fig.11 Flexure Failure Specimens Subject to Anti-symmetrical Bending

3) The strength of shear failure beams in experiments are generally a little smaller than that of the theoretical one.

4) Though the diagonal compression field is supposed to be formed only in a "short" beam-column intuitively, this theory predicts the ultimate strength fairly well without affected with the change of the parameter ℓ/D.

5) The accuracy of the theory is not also affected with parameter F_c, though it is often considered that the shear strength is the function of $\sqrt{F_c}$ and not F_c.

6) Though this analysis over-estimates the resistance of a shear bond failure specimen a little, coefficient of variation σ/m for Q_e/Q_c is small. small.
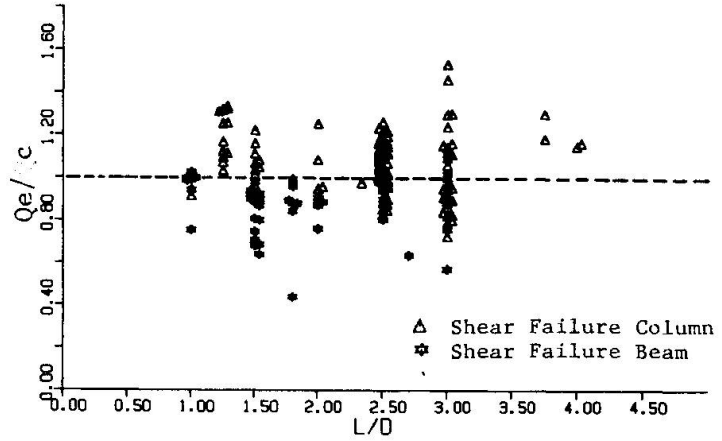
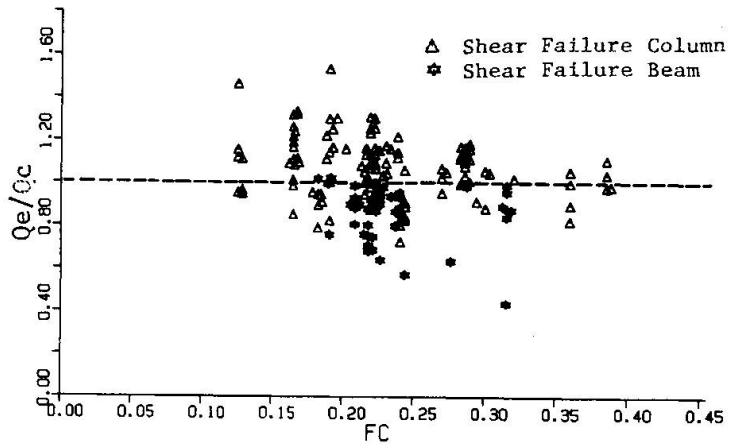Fig.12 Shear Failure Specimens Subject to Simple beam type Loading

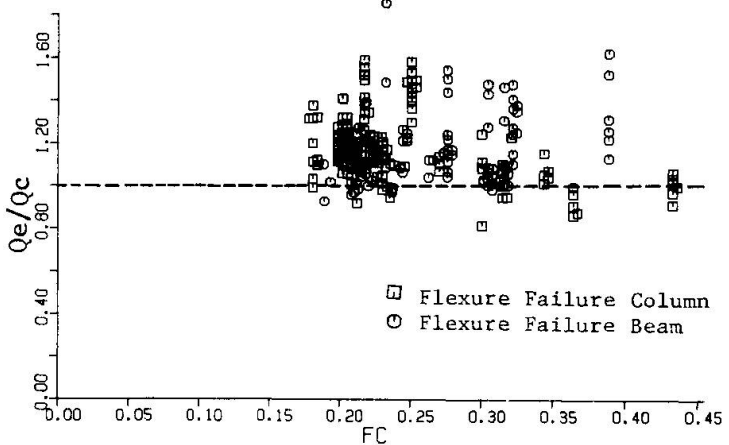Fig.13 Shear Failure Specimens Subject to Simple Beam Type Loading

Fig.14 Flexure Failure ecimens bject to Symple Beam Type Loading

3.2. Ultimate Strength of Reinforced Concrete Member Subject to Shear and Axial Force without Bending

The Experimental results tested using the loading apparatus shown in Fig.7 and writers' prediction by Eq.33 are shown in Fig.15.

Marks $\circ$ $\bullet$ show the test results by Mattock et.al.[2]and marks $\triangle$ show the test results by Aoyagi[4] et. al.

Though the theoretical prediction by Eq.33 show a fairly good correlation to the test results, it overestimates the resistance perhaps due to the fact that the plastic stress can not be sufficiently redistributed in such an extremely short length of specimen. A reduction factor of 0.78 may be applied to Eq. 33 to obtain the modified semi-empirical formula which is shown by dashed line in Fig.15.
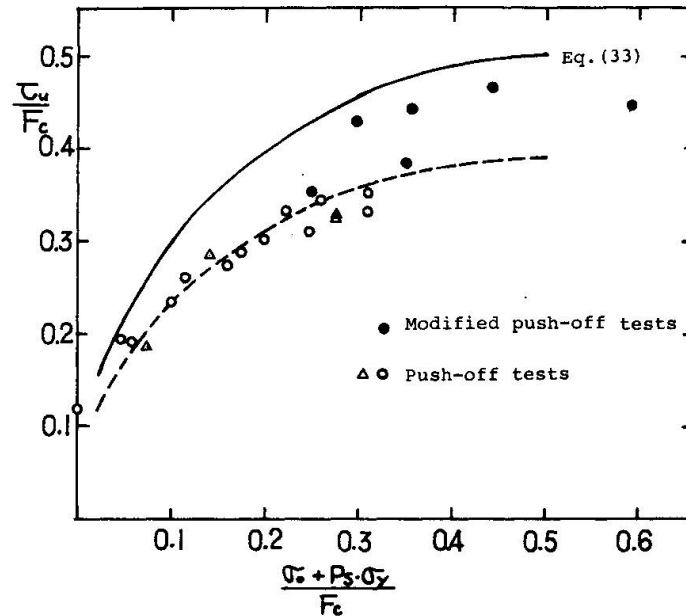

Fig.15 Comparison Between Test Results and Calculated Values

4. CONCLUSION

The ultimate strength of reinforced concrete members was analyzed based on the concept of compression field. In this analysis, the interaction among bending moment, axial force and shear force was evaluated using a simple mathematical model. Though proposed theory is simple, it can explain the test results of reinforced concrete beam-columns and precast concrete connections fairly well on a unified theory.

REFERENCES

[1] Hirosawa "Strength and Ductility of Reinforced Concrete Members", Report of the Building Research Institute No.76 (in Japanese)

[2] Mattock, Hawkins, "Shear Transfer in Reinforced Concrete Recent Research" PCI Journal/ March-April 1972

[3] Architectural Institute of Japan, AIJ Standard for Structural Calculation of Reinforced Concrete Structures, 1971 (in Japanese)

[4] Aoyagi et.al., "Full Scale Model Push-off Test of Reinforced Concrete Block with 51 mm dia. Deformed Steel Bars", Trans. of the 6th International Conference on Smirt J/4/7 1981